

Fractographic Studies in Ballistically Damaged Polycrystalline Alumina

Chong-Hee Kim

Dept. of Materials Science, KAIS

(Received May 7, 1978)

탄도충격으로 파괴된 다결정 Alumina의 파면조직

김 종 희

한국과학원, 재료공학과

(1978년 5월 7일 접수)

초 록

탄도충격에 의하여 파괴된 다결정 alumina의 파면조직을 광학 및 투과 전자현미경으로 연구 분석하였다. 파면의 주된 파괴 양상은 결정 입개면의 불리 또는 결정입내 파괴로 구성되어 있고 이러한 파괴과정은 복잡한 cleavage 양상과 결정입자 내에서의 소성변형을 수반하고 있다. 미세조직 관찰 결과에 의하면 alumina ceramics의 충격 파괴 과정에서 에너지의 흡수가 극부적인 소성변형으로 나타나고 있음을 알 수 있었다.

INTRODUCTION

Since most ceramics fail by a fracture process, a detailed study of fracture mechanisms in ceramics will contribute a great deal in understanding the failure of ceramics, especially under impact conditions. In the case of polycrystalline ceramics, fracture behavior is complicated by grain size and shape, porosity, and impurity content. Their distributions, the applied stresses, and test conditions will give rise to further complications in its behavior.

Optical microscopy is limited to the low magnification study of such fracture surfaces because of the limited depth of focus and low resolving power of an optical microscope. Since most fracture surfaces are very rough, the depth of focus is of major importance in fractography. The restricted depth of focus of an optical microscope limits its use to low magnification ranges only.

Detailed examinations of fracture surfaces at higher magnifications has to be accomplished by other means.

Replication electron fractography has come to prominence during the past decade for the detailed examination of fracture surfaces at high magnification; however, it allows only an indirect examination of the fracture surfaces. The preparation of a shadowed replica of a fracture surface usually involves a one-, two-, or three-step process which is usually very time-consuming and requires great skill. In addition, artifacts not associated with the fracture phenomena are often produced.

The present work, employing two microscopic techniques, is aimed at a basic understanding of the mechanisms contributing to generation of fine textures on sheared, spalled and cracked polycrystalline alumina surfaces produced by ballistic impact events.

MATERIALS AND PROCEDURES

A ballistically damaged specimen of commercially produced polycrystalline alumina ($\sim 94\%$ α - Al_2O_3) was obtained for this study from other investigators concerned with impact resistance of potential light armor materials. The specimen, originally measuring $6'' \times 6'' \times 3/8''$, had been cemented to, and was supported by, fiber-reinforced backing material. During armor testing, it had been struck by a 0.30 caliber armor piercing projectile at a velocity sufficient to cause severe damage and penetration (Fig. 1).

The fracture surface being investigated was cleaned with acetone to remove dust or other foreign materials. Surface residues and tiny fracture fragments then were

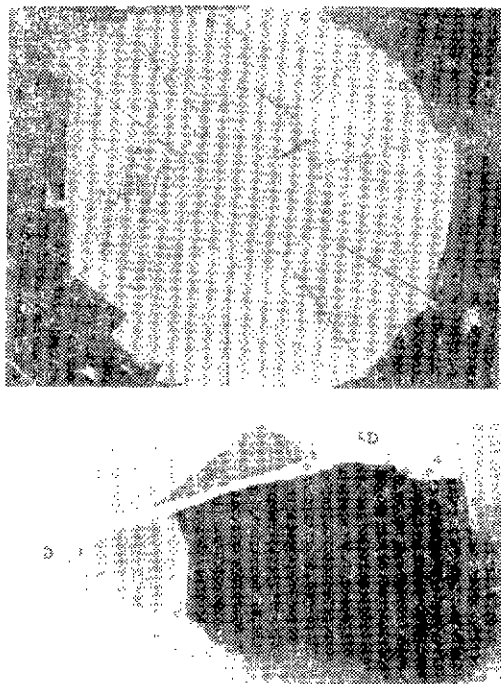


Fig. 1 Ballistically damaged polycrystalline alumina.
 a. Back face of tile after removal of spalled material, X1.6. Numbers identify areas from which surface replicas were taken.
 b. Detail of shear conoid surface (arrow) and radial crack for segment D, X1.4.

removed by applying, stripping, and discarding plastic replicating tape two or three times in succession. Thereafter, a small amount of the replication solution was dropped on the area selected for study and allowed to spread on the surface of the specimen. Replicating tape was applied smoothly over the coated area avoiding bubble entrapment. Light, uniform pressure was applied to the tape during the 3-5 minutes required for evaporation of the solvent.

With tweezers, the replicating tape was carefully stripped off and transferred to a glass microscope slide surfaced with double backed transparent tape. A slide containing many such first replicas was then processed in vacuum coater to produce shadowed carbon second replicas.

The replicas were shadowed with an evaporated thin film of platinum ($<100 \text{ \AA}$) impinging at 30° for the single crystal replicas and at 45° for polycrystalline replicas.

An evaporated film of amorphous carbon thin enough to be transparent to electrons and strong enough to constitute the second replica was thereafter deposited at an incident angle of 90° without intervening atmospheric exposure.

The shadowed replica film was then cut to fit $1/8''$ diam specimen support grids, and floated in acetone to dissolve the initial plastic replica. Within 15 to 30 minutes, depending on the thickness of the replicating tape, the plastic was fully dissolved. Completion of this phase was evident when the platinum shadowed carbon second replica sank to the bottom of the container. The replica was retrieved from the solvent on a copper specimen grid, and allowed to dry by evaporation.

This procedure produced satisfactory replicas of polycrystalline aluminum oxide fracture surfaces. Replicas representing selected areas of fracture surfaces were examined and photographed at appropriate magnifications in a JEOLCO JEM-120 transmission electron microscope at 80 kv.

RESULTS AND DISCUSSION

The best available information¹⁻³, suggests that damage produced by an impacting projectile in a polycrystalline

¹ Specimen provided by Capt. McDonald Robinson, Ceramic Laboratory, U.S. Army Mechanics and Materials Research Center, Watertown, Mass.

ceramic occurs in at least four successive stages, with each stage being identified with a particular fracture geometry, stress configuration, and energy spectrum. In an approximate, decreasing order of the total system energy remaining to be dissipated, these stages result in (1) comminuted particulates from within a shear conoid whose axis is the impact trajectory, (2) fracture surfaces associated with the shear conoid interface, (3) radial cracks whose surfaces are approximately parallel with the impact trajectory, and (4) late-phase spall cracks whose surfaces are almost perpendicular to the impact trajectory.

Comminuted material from the first category was not available for this study, but representative replicas of each of the three subsequent stages of fracture were prepared at selected positions as indicated in Figs. 1a and 1b. Subsequent sections present microstructural and fractographic information obtained from these replicas.

Conoid Shear Surface

Very little of the principal conoid shear surface was available for study. The replicated surface examined in this study was obliquely oriented (45°) with respect to the impact trajectory (see Fig. 1b). Fig. 2 illustrates several features characteristic of this heavily damaged surface. Fracture was predominantly transgranular, and was rather direct, producing relatively flat, fan-shaped river patterns, some of which show multiplications of river pattern components as the fracture front traverses subgrain or grain boundaries⁴. In many instances, progressions from one grain to the next appear to have required considerable shear damage before the crack could be freed to proceed ahead in river pattern cleavages or intergranular separations. Within these sheared regions, distinctly localized and heavily concentrated groupings of small bumps or protrusions have been noted. Their origin has not been clearly established, but they appear to suggest locally intense deformation processes akin to the early stages of microvoid development during plastic fracture in metals⁵⁻⁷. Alternatively, adiabatic heating associated with shockwaves generated by ballistic impact may have been sufficient to melt glassy phase material (~ 16 vol %) in this alumina body such that molten glass was either extruded from or spattered onto fracture surface.



Fig. 2 Complex fractography of conoid shear surface in ballistically damaged polycrystalline tile. Two stage plastic-carbon replica, Pt-shadowed at 30°

This early phase of fracture is marked by a very considerable number of fracture fragments (small, dark shards) which have been extracted in situ by the replication process. These fragments suggest that branching and/or multiple cracks were not uncommon at this stage of impact energy absorption.

Strong association of fragments with sheared regions suggests that locally intense plastic processes may have played a significant role in their formation. Examinations of some of these fragments in direct transmission have revealed high concentrations of dislocations⁸.

Radial Crack Surfaces

Radial cracks apparently begin to propagate during an impact event at a time after the shear conoid has been well established; their formation is probably concurrent with dissipation—by several processes—of a substantial part of the total impact energy. The innermost portions of the primary radial cracks are relatively smooth, and are thought to be generally similar in terms of fractography to the conoid shear surfaces

described above. The main run of the cracks develop very rough surfaces, with complex textures whose elemental "wave forms" have amplitudes and periods extending over an estimated 10^2 - 10^3 grain diameters. Final portions of such cracks, especially if diverted or offset, tend to become relatively smooth again.

Figures in this section show fractographic details at three different radial distances along one radial crack: at point 3 (Fig. 1b) $\sim 2.8''$ from the point of impact, in a region of heavy, rough texturing; at point 4 $\sim 3.7''$ from the center on a more smoothly textured, predominantly conchoidal surface produced by the main crack after it had undergone an abrupt offset (0.2 in.) (Fig 3-4); and at point 5, on a relatively smooth transverse crack (a secondary crack almost normal to the main crack) at a distance of $3.9''$ from the point of impact (Figs 5-6).

Rough Surfaces The fractograph in this section shows that heavily stepped fracturing (typically based on

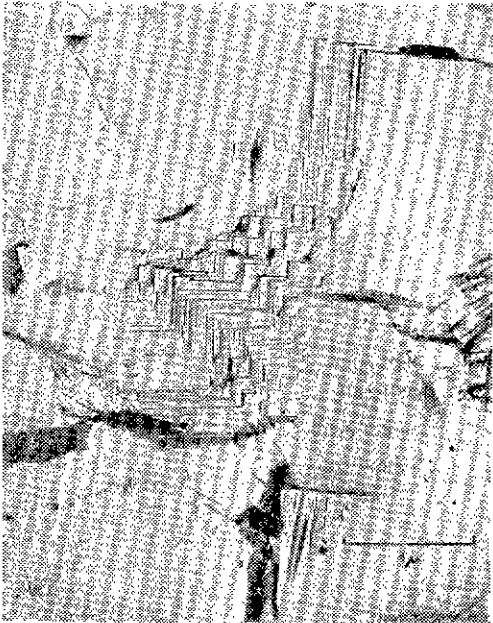


Fig. 3 Intergranular separations, transgranular cleavage steps, conchoidal fractures and in situ fracture fragments contribute to the very complex topography of a smoothly textured portion of a radial crack in ballistically damaged polycrystalline alumina tile. Two stage plastic-carbon replica, Pt-shadowed at 30° .

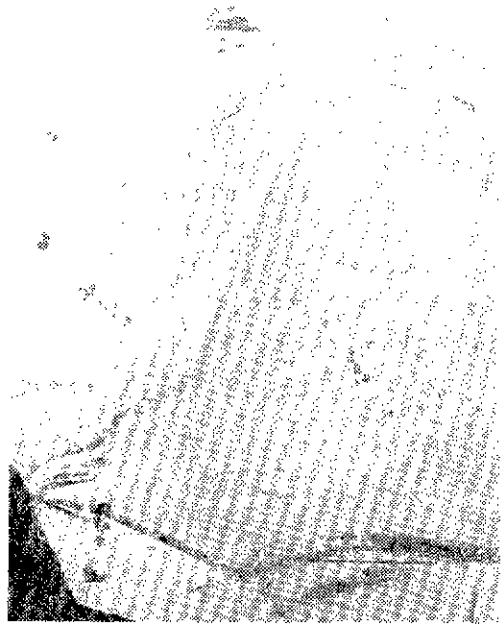


Fig. 4 Transition from intergranular separation to transgranular fracture along grain edge junction on a radial crack surface in ballistically damaged polycrystalline alumina tile. Two stage plastic-carbon replica, Pt-shadowed at 30°

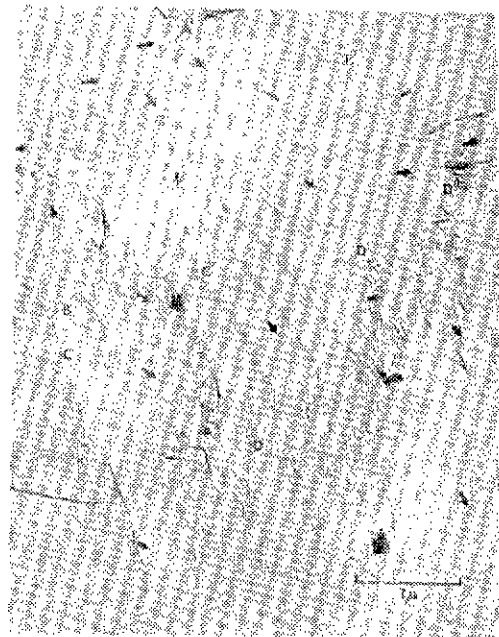


Fig. 5 River pattern cleavage steps on transverse secondary crack in ballistically damaged polycrystalline alumina tile. Two stage plastic-carbon replica, Pt-shadowed at 30° .



Fig. 6 Interactions between cleavage cracks and microstructural features on transverse secondary crack surface in ballistically damaged polycrystalline alumina tile. Two stage plastic-carbon replica, Pt-shadowed at 90° .

intersections of two 1st and one 2nd order rhombohedral cleavage planes⁹) constitute one significant fracture mode in the rough portions of radial cracks. Intergranular separations also have been observed to be quite prominent in the still incomplete investigations of this experimentally difficult fracture category. Only scanning electron microscopy (combining moderate to high magnification, high resolution, and extreme depth of focus) is likely to provide adequate characterizations of such rugged but finely detailed surfaces.

Smoother Radial Crack Surfaces Though the fracture surface was relatively smooth in the macroscopic sense, fractographs taken from this region illustrate the extremely complex nature of surfaces produced by highly localized combinations of almost every possible fracture mode. Transgranular conchoidal fracture is more prominent than in the previous examples. The curving conchoidal fractures are neither smooth nor uniformly textured. Rather, they contain an abundance of fine detail which suggests that the advancing crack was sensitive either to progressive changes in crystallographic orientation, or in local states of stress and strain, or

both, very high surface energies ($\gamma_f \geq 40,000$ ergs/cm²) were associated with non-planar fracturing (i. e., conchoidal) in Wiederhorn's attempts to cleave basal planes in sapphire⁹. The conchoidal surfaces illustrated here appear to provide many evidences of stubborn resistance to separation. In comparison to essentially brittle cleavages, they appear to have been produced by cracks which had been subjected both to some blunting and to continuous redirections; such textures are not inconsistent with very large fracture surface energies.

In Fig. 3, conchoidal fractures, intergranular separations, two very characteristic forms of rhombohedral cleavage, and several examples of fracture fragment formation are illustrated. The central grain shows a very well defined shift from intergranular separation to transgranular cleavage. In Fig. 4, the long central boundary surface shows a distinct transition from boundary separation on the right (which grades off into parting and conchoidal fracture) to transgranular fracture on the left. Of particular interest is the strong redirection of the transgranular fracture (just to the left of the boundary trace) together with the unusual sheared appearance at the left of the boundary flat. Such a configuration possibly is associated with some grain boundary sliding¹⁰ at a constrained triple grain edge, causing a small amount of shear. Relaxation of the strains imposed by a sliding mechanism would require either generalized plastic deformation or transgranular fracture of one or more of the adjacent grains, as observed here.

Smooth Transverse Fractures The surface studied in Figs. 5-6 is considered to be a secondary crack (probably a consequence of reflected stresses) and thus may be representative of a relatively late portion of the fracture time sequence, and hence of a proportionally lower segment of the energy dissipation spectrum. The principal fracture features include both grain boundary separations and transgranular breaks, together with generation of fine fracture fragments. The transgranular portions range in texture from conchoidal to imperfect parting to well defined cleavage. The orthogonally stepped cleavage mode commonly observed on single crystal fracture surfaces and on primary radial cracks in this polycrystalline material is less evident in this

secondary crack. The intensity of texturing is significantly reduced from the more severe cases previously cited. At the higher magnification provided by Fig. 5, there are several interesting examples of interactions between the advancing crack and the crystalline substructure (principally subgrain boundaries). Multiplications and redirections occur at the grain boundary marked by line A-A', other changes along B-B', C-C', D'-D'', B'-D' may be indicative of the influence of subgrain boundaries. These interactions apparently result in very local alterations of the fracture texture, as noted by Low⁴.

Some interesting examples of interactions between advancing cleavage cracks and microstructural features are shown in Fig. 6. Angular grain boundaries (A) at the upper right are typical of polyphase ceramic bodies which rely in whole or in part upon liquid phase sintering¹¹⁻¹³. The crack was not significantly altered in perpendicularly traversing these thickened (presumably vitreous) boundaries should produce hackled, splintered and/or conchoidal textures typical of fracture in glassy materials¹⁴.

After changing from boundary separation to transgranular fracture at (B), the crack produced finely textured but very irregular stepped cleavage fractures in moving toward pore (C). Since the nearby and nearly parallel grain boundary (D) appears to have been already separated, it may be that these cleavage anomalies resulted from stress relaxation associated with the separated boundary, coupled with the normal resistance to cleavage within the grain and at its other boundaries. At the pore (C) several changes in fracture behavior can be noted, both in the immediate pore vicinity, and at longer distances extending to the end of the grain. Related fracture tails at microstructural discontinuities in ceramics and glasses have been reported elsewhere¹⁵⁻¹⁶.

The downstream tailing effect is less prominent for the faceted pore (E), but the pore possibly did cause the unusual cleavage perturbations oriented in a perpendicular direction at (F). The discontinuity represented by the pore may have caused stresses associated with the crack front to be resolved into new components, including those capable of producing this anomaly.

Late-Phase Spall Cracks

This category of fracture damage, though prominent in terms of total exposed area (see Fig. 1a), is thought to be representative of the final stages of cracking, occurring at the time when the kinetic energy of impact has been substantially dissipated. Both transgranular and intergranular fracture modes are observed. Cleavage is the most characteristic process for transgranular fracture, but the roughness of texturing is not as severe as in the earlier stages of fracture. Significantly, there is very little evidence of fracture fragments of the sort which were common on more severely damaged surfaces.

From all these observations, it is apparent that the fracture process in polycrystalline alumina is not purely brittle. Instead, energy is absorbed during the propagation of fracture by any of several (often combined) processes, namely, secondary crack formation, localized plastic deformation, areal increases due to fracture surface roughness, and/or step formations which lead to high-energy tearing fracture¹⁷.

SUMMARY AND CONCLUSIONS

Microscopic evidences from replication fractography strongly support the concept of localized plastic deformation processes associated with fracture resulting from ballistic impact events in polycrystalline alumina. The microstructural features are in large part those typical of nominally brittle fracture in polycrystalline material; fracture surfaces are mainly composed of a combination of transgranular and intergranular regions. This indicates that the crack propagation mechanism is complex; it was necessary to propagate discontinuously, starting new cracks in succeeding grains. Such a process will tend to reduce the velocity of crack propagation and ultimately will stop crack advancement, unless high stress states are sustained by external loading. While the main crack propagates, bursts of easy cleavage spread ahead, become arrested and are reinitiated. Propagation of cleavage microcracks commonly results in the formation of complex cleavage facets, river patterns, and secondary cleavage, coupled with plastic tearing within individual grains. Relatively easy cleavage processes spread forward and laterally through favorably oriented grains ahead of the main crack front; however, if the main crack is to advance, additional energy must

be supplied by the available elastic strain energy. Some of it, an additive factor over and above the simple surface energy, clearly is absorbed in the process of forming these fine extra textures.

The almost inescapable conclusion to be drawn from these findings is that truly brittle cracks—those which can be propagated with fracture surface energy (γ_f) comparable to the calculated surface free energy (γ_s) without doing work upon the bulk of the material traversed—are relatively rare in this refractory oxide. Rather, the fractures commonly observed in aluminum oxide were propagated (at least in part) as blunted cracks—those in which the fracture surface energy (γ_f) has been substantially increased above the nominal free energy (γ_s) because of plastic work energy (γ_p) which had to be expended in deforming bulk material at and near the advancing crack front.

Fracture surface energies in alumina ranging from approximately 25,000 to 50,000 ergs/cm² have been reported by several investigators. Numerical values generally have been based upon calculations incorporating only the projected crack surface area¹⁷. Actual surface areas have been considered to be as much as three times greater than projected areas¹⁷, an estimate which is considered to be realistic in terms of the fractographic examinations made during the present study. If the reported gross values for γ_f are normalized with respect to actual surface areas [i. e., divided by the suggested factor of three], the range for resultant net fracture surface energy (γ_{f0}) is from approximately 8,350 to 16,700 ergs/cm². The net values are still some seven to fifteen times larger than calculated surface free energy values ($\gamma_s \approx 1136$ ergs/cm²)¹⁸. For polycrystalline alumina of moderate grain size, these rather conservative estimates [$\gamma_p = \gamma_{f0} - \gamma_s$] yield γ_p values ranging from about 7,200 ergs/cm² to more than 15,000 ergs/cm². For this nominally brittle ceramic material, the Orowan criterion for a plasticity component in fracture, $\gamma_p > \gamma_s$, seems well satisfied, in good agreement with the microscopic evidences of yielding presented here. Finally, it should be noted that these findings, based upon high velocity ballistic damage events, are also in good accord with those reported by Congleton, et al¹⁹ for slow single stroke fractures in alumina.

LIST OF REFERENCES

1. D.M. Martin; p. 5-12 in *Ceramic Armor Technology*, Edited by J.C. Dunleavy and W.H. Duckworth (DCIC Report 69-1, Part I). Battelle Memorial Institute, Columbus Ohio, (1969)
2. C.F. Cline and M.L. Wilkins; p 13-18 *ibid*
3. V.D. Frechette and C.F. Cline, "Fractography of Ballistically Tested Ceramics", *Amer. Ceram. Soc. Bull.* **49** (11) 994-997, (1970)
4. J.R. Lew, Jr.; p 68-90 in *Fracture*, Edited by B.L. Averbach, D.K. Felbeck, G.T. Hahn, and D.A. Thomas, John Wiley and Sons, Inc., New York, (1959)
5. C. Crussard, J. Platcau, F. Tamhanker, G. Henry, and D. Lajeunesse; p 524-561, *ibid*.
6. C.D. Beachem, "An Electron Fractographic Study of the Influence of Plastic Strain Conditions upon Ductile Rupture Process in Metals". *Trans. Am. Soc. Metals.* **56**, 318-326, (1963)
7. C.D. Beachem and D.A. Meyn, "Illustrated Glossary of Fractographic Terms, Section 2, Glide Plane Decohesion, Serpentine Glide, Ripples, Stretching, Microvoid Coalescence". NRL Memorandum Report 1547, June 1964.
8. H. Palmour III, C.H. Kim, D.R. Johnson, and C.E. Zimmer (N.C. State Univ.). "Fractographic and Thermal Analysis of Shocked Alumina", Technical Report 69-5, THEMIS Research Program on Materials Response Phenomena at High Deformation Rates, Contract N00014-68-A-0737. p 97, April 1969.
9. S.M. Wiederhorn, "Fracture of Sapphire". *J. Amer. Ceram. Soc.* **52** (9), 485-491. (1969)
10. S.C. Carniglia; p425-472 in *Materials Science Research*, vol. 3, Edited by W.W. Krieger and H. Palmour III, Plenum Press, New York, (1966)
11. (a) W.D. Kingery, "Densification During Sintering in the Presence of a Liquid Phase: O. Theory", *J. Appl. Phys.* (3) 301-306. (1959)
(b) W.D. Kingery and M.D. Narasimhan, "Densification During Sintering in the Presence of a Liquid Phase: II. Experimental", *ibid.*, 307-310

- (c) W. D. Kingery; p 386-389 in Introduction to Ceramics, John Wiley and Sons, Inc., New York, (1961)
- (d) W. D. Kingery; p 187-194 in Kinetics of High Temperature Processes, The Technology Press of M. I. T. and John Wiley and Sons, Inc., New York, (1959)
- (e) W. D. Kingery; p 131-143 in Ceramic Fabrication Processes, The Technology Press of M. I. T. and John Wiley and Sons, Inc., New York, (1960)
12. R. L. Coble; p 213-228 in Ceramic Fabrication Processes, Edited by W. D. Kingery. The Technology Press of M. I. T. and John Wiley and Sons, Inc., New York, (1960)
13. D. B. Binns and P. Popper, "Mechanical Properties of Some Commercial Alumina Ceramics", *Proc. Brit. Ceram. Soc.* **6**, 71-82, June 1965
14. (a) E. F. Poncelet, "Fracture and Comminution of Brittle Solids", *Trans. A. I. M. E.* **169**, (1946)
 (b) E. F. Poncelet, "The Mechanism of Fracture Propagation", Technical Report, Poulter Laboratories of Stanford Research Inst., Menlo Park, Calif., July 1963.
15. H. Palmour III, D. M. Choi, L. D. Barnes, R. D. McBrayer, and W. W. Kriegel; p 158-197 in Materials Science Research, vol. 1, Edited by H. H. Stadelmaier and W. W. Austin, Plenum Press, New York, (1963)
16. S. N. Ohlberg, H. R. Bolob, and C. M. Hollabaugh, "Fractography of Glasses Evidencing Liquid-in-Liquid Colloidal Immiscibility", *J. Amer. Ceram. Soc.*, **45** (1), 1-4, (1962)
17. (a) F. J. P. Clarke, H. G. Tattersall, and G. Tappin, "Toughness of Ceramics and Their Work of Fracture", *Proc. Brit. Ceram. Soc.* **6**, 163-172, June 1966
 (b) H. G. Tattersall and G. Tappin, "Work of Fracture and its Measurement in Metals, Ceramics and Other Materials", *J. Mater. Sci.* **1** (3), 296-301, (1966)
18. R. H. Bruce; p 359-367 in Proceedings of the Second Conference held under auspices of the British Ceramic Society and the Nederlands Keramische Vereniging at Noordwijk aan Zee, Edited by G. H. Stewart, Academic Press, (1965)
19. (a) J. Congleton, M. R. Holdsworth, and N. J. Petch, "The Brittle Fracture of Alumina", Final Technical Report, European Research Office, United States Army, Contract Number DAJA 37-67-C-0522, University of Newcastle upon Tyne, United Kingdom, (1968)
 (b) J. Congleton, N. J. Petch, and S. A. Shields, "The Brittle Fracture of Alumina Below 1000°C", *Phil. Mag.* **19**, 795-807, (1969)